

An experimental study of Froude number effect on wind-tunnel saltation

B. R. White and H. Mounla, Davis, CA, U.S.A.

Summary. The simulation of the natural process of saltation in a wind tunnel is considered. The pioneering interactive boundary-layer analysis of Owen and Gillette [11] concluded that an independence Froude number criterion did apply to the problem and they estimate, based on wind-tunnel Froude number data ranging from 35 to 80, an independence Froude number value of about 20 for saltating flows to be free of facility constraints imposed on the saltation. The present experimental flows had Froude numbers ranging from about 6 to 1000. Analysis of friction speed variation as a function of downstream position suggests a more conservative critical Froude number value of 10 be used. Also, there appears to be an additional requirement, for most of our data, that tunnel's downstream length-to-height ratio be greater than 5. Therefore, a maximum Froude number of 10 and minimum tunnel length-to-height ratio of 5 is suggested to insure accurate saltation tunnel simulation.

1 Introduction

This study expands upon the work by Owen and Gillette [11] and Owen [10], which sets operation limits on wind tunnels, and analyzes variation of the friction speed as a function of the downstream position for various Froude numbers in the presence of a saltating particle bed. The dimensions of the wind tunnel are important factors in determining if a choked saltation flow will occur, resulting in a blockage of the airflow. Under choking conditions, particle flux and velocity profiles are altered by the constraints placed upon the flow by the wind tunnel. Thus, inaccurate modeling will occur. According to Owen and Gillette, a wind tunnel operated at a speed which has a value of the Froude number less than 20, should be free from this effect, resulting in small variations of u_* as a function of the downstream position.

The wind-tunnel experiments, carried out by Owen and Gillette, were for a relatively small tunnel (19.5 cm high) where the determinate influence of Froude number was readily noticeable. Their experimentally determined values of Froude number were all in excess of 35 or almost double their recommended maximum value of 20 for flows to be free of Froude number effects. In observing Fig. 4 of their paper, it may be noticed that few, if any, of the saltating flows achieve a constant value of friction speed u_* with downstream distance. This result is to be expected since the Froude number independence principle (i.e., Froude number values less than 20) was not met in their experiments.

One of the main objectives of the present study was to carry out windtunnel experiments in which the Froude number criterion was met and then determine with a relatively high degree of accuracy the variation of u_* as a function of both downstream distance and Froude number. If the Froude number criterion is met and the tunnel is free of entrance effects,

then u_* should approach or obtain a constant value. Accordingly, saltation experiments have been conducted in a UC Davis boundary-layer wind tunnel and in NASA's low-pressure MARSWIT wind tunnel that have produced a range in Froude number from about 6 to 1000. Thus, we were able to test the hypothesis of the Froude number independence principle over a wide range of Froude numbers.

Lastly, many mathematical formulations predicting mass transport rates (the mass of particles, M , passing through a finite width, w , during a time interval T) are found in the literature (a nice summary of these formulae is found in Greeley and Iversen [3]). Nonetheless, a limited number of these expressions are more favored than the others, as they are considered more accurate. The reason for the discrepancy in wind-tunnel measurements of transport rates is, in part, attributed to the collector's efficiency, which is a function of the wind tunnel as well as aerodynamic features of the collector's shape. Therefore, it is of importance to determine an efficient particle collector for any tunnel. The present study summarizes the results of such an investigation; i.e., the optimum particle collector was determined experimentally for the UC Davis boundary layer wind tunnel. Additionally, mass flux as a function of height as well as total mass fluxes were measured. Simultaneous measurements of the mass flux rate along with velocity profiles at the same location were also made.

2 Wind-tunnel facility and measurement techniques

The majority of the saltation experiments were performed in a boundary-layer wind tunnel located at UC Davis shown schematically in Fig. 1. The tunnel was designed to simulate particle flow in saltation, and it consisted of four major sections: (i) entrance, (ii) flow development, (iii) test, and (iv) diffuser. The overall length of the tunnel was 13 m.

The entrance section consisted of a 0.48 m long contraction area having a ratio of 5:1 equipped with honeycomb flow-straighteners to reduce the freestream turbulence level. The 7.32 m flow development section had diverging walls and was composed of three individual sections which were each 2.44 m (8 feet) long made of plywood. The Plexiglas test

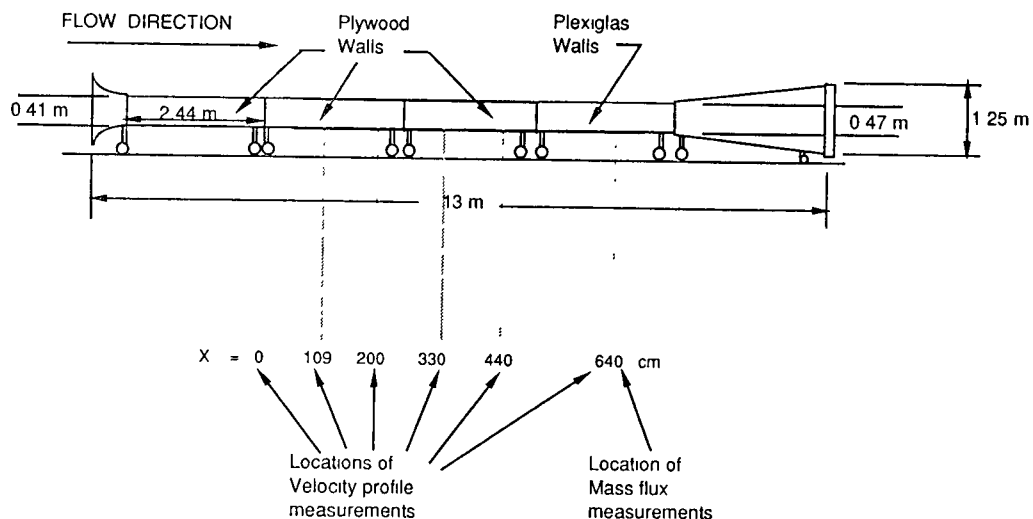


Fig. 1. Schematic of the wind-tunnel facility at the University of California, Davis

section was 2.44 m in streamwise length and 0.47 m high by 0.8 m wide in cross section. The diffuser, 2.8 m in length, had an expansion area ratio of 13:1 which provided a continuous transition from the rectangular cross section of the test section to a circular cross section for the fan.

The tunnel was equipped with a 3 hp, variable speed *DC* motor that rotated an 8-blade fan. An *AC/DC* power converter supplied power to the motor, and had controllable air speed inside the tunnel of up to 15 m/s.

3 Mean velocity profiles in saltation

A series of experiments, in the presence of saltating particles, were carried out to measure the mean velocity profiles and determine the effect of Froude number on the upstream of the bed. The Froude number was defined as $U_1^2/(gH)$, where U_1 is the inviscid uniform velocity upstream of the bed, g is the gravitational acceleration and H is the tunnel height.

A 1 cm deep smooth bed of walnut shells was placed on top of the nonerodible walnut shell surface. The bed started 2.4 m downstream from the entrance and extended about 7.5 m downstream to the end of the test section.

A Pitot-static tube, mounted on a transversing mechanism, moved vertically from the floor of the tunnel upward to a height of 31.2 cm to determine the mean velocity probe.

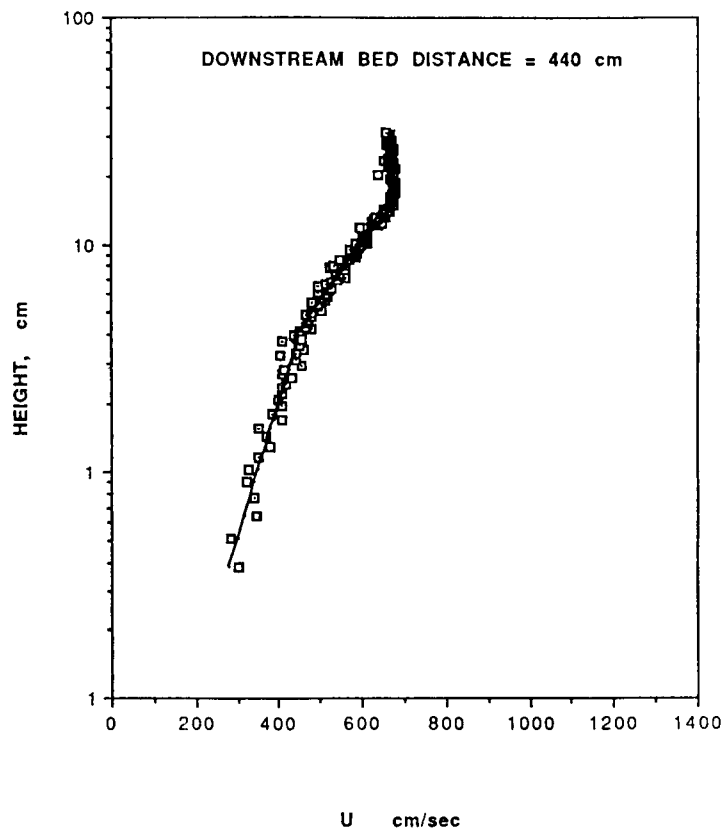


Fig. 2. Typical measured velocity data (240 values) as a function of logarithmic height. The two solid lines represents a linear regression fit to the data

The Pitot-static tube was connected to the Barocel pressure system which in turn was electronically connected to an A/D system controlled by an IBM AT PC. The data acquisition system operated at a rate of 1000 Hz and the program averaged 500 pressure readings acquired in 0.5 seconds to yield one data point of the velocity profile. Each profile consisted of 240 time-averaged individual points. A single profile required two minutes to be measured. Figure 2 displays a typical profile acquired at a downstream distance of 6.84 m from the entrance with a freestream speed of 6.46 m/s.

The aerodynamic roughness height of the loose bed of material was determined by measuring several velocity profiles, each at a different freestream speed, all below threshold condition. The value of the surface roughness was found to be 25 microns.

4 Determination of friction speed in saltation

The friction speed, u_* , in the presence of saltating particles, could not be determined by using the simple slope method, because of the ambiguity in the velocity profile. However, when the wake region is accounted for in much the same manner as Coles' law-of-the-wake [2] equation for smooth-wall turbulent boundary layer case a reasonable estimate of u_* may be obtained.

Therefore, the rough-wall case, with saltation occurring, may be represented by

$$\frac{u}{u_*} = \frac{1}{k} \ln_e (y/y_0) + \frac{\Pi}{k} (1 - \cos (\pi y/\delta))$$

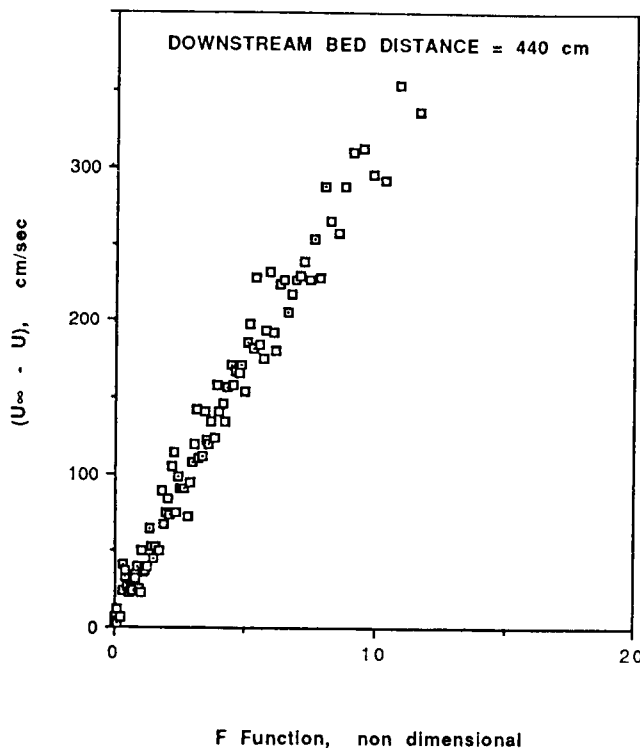


Fig. 3. The deflected velocity as a function of F . The mean slope of the data is equal to the friction speed

where k is von Karman's constant, equal 0.418; and H is Coles' wake parameter which is a function of pressure and momentum-deficit Reynolds number; here it is assumed equal to 0.55 (White [13])

Applying this relation at the edge of the boundary layer and at an arbitrary location within the boundary layer yields (subtracting one from the other according to Mounla [8]),

$$\frac{u_\infty - u}{u_*} = \frac{-1}{k} \ln(y/\delta) + 1.32(1 + \cos(\pi y/\delta)) = F$$

or

$$u_\infty - u = u_* F$$

Note, the form of the rough-wall velocity defect, $u_\infty - u$, is essentially the same as the smooth-wall case, since the additive constant in both cases disappears when the difference of u_∞ from u is taken.

Figure 3 presents the difference between the freestream velocity and the instantaneous velocity within the boundary layer as a function of F . The slope of this plot corresponds to the friction speed. Thus, the friction speed may be determined from the velocity profiles measured during saltation. This calculation is needed to determine the constancy of u_* with downstream position and Froude number.

5 Composite mean velocity profiles in saltation

Composite mean velocity profiles were measured during saltation at different locations along the tunnel to determine the friction speed variation as a function of downstream location. To insure uniform test conditions, at the end of each previous run, the particle bed was reconditioned to its original 7.5 m length and position, by replacing particles over the eroded portion of the surface and again smoothing it. The bed length had to be maintained constant, since the variation of the friction speed as function of the downstream location was to be investigated.

The mean velocity profiles (logarithmic height versus speed), in the presence of saltating particles, follow a straight line from the surface and then experience a deflection point at a certain height to follow another straight line to the edge of the boundary layer. Figure 4 displays the composite profiles (A , B , C , and D on each figure) at downstream bed positions of 1.1, 2.0, 3.3, 4.4, and 6.4 meters from the beginning of the bed. The lines plotted are linear regressions determined from the actual velocity profile data (such as the linear regression lines displayed in Fig. 2). Great care was taken to match the two segments of each profile at their interface as well as match the local freestream speed, u_∞ , above the boundary layer. The inviscid upstream velocity for each of the profiles A , B , C and D was held constant for each downstream profile measurement; note however, locally, the freestream values of the curves A , B , C and D changed as a function of downstream position. Table 1 presents this information. The value of the threshold friction speed for the walnut shell, at a downstream distance of 640 cm was found to be 22.5 cm/s.

Over a non-saltating rough surface, the mean velocity profiles for different speeds as functions of logarithmic height theoretically coalesce at a focus point (at zero speed) to define the roughness height y_0 , as given in the relation,

$$\frac{u}{u_*} = \frac{1}{k} \ln_e(y/y_0)$$

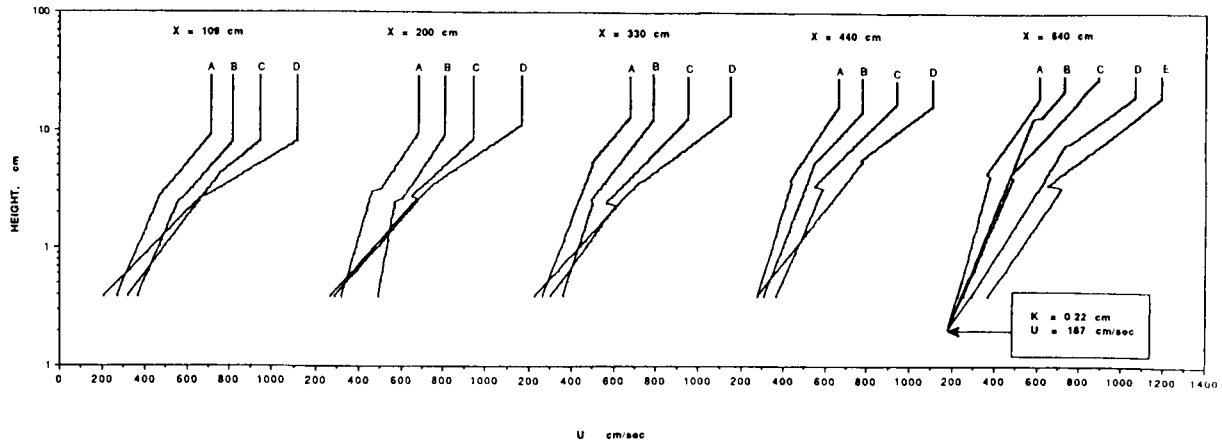


Fig. 4. Composite velocity profiles as a function of logarithmic height. The solid lines are linear regressions of the individually measured profiles. The individual values of friction speed are found in Table 1, except for curve *E* at downstream position 640 cm, which had a friction speed of 70 cm/s

Table 1. Calculated values of friction speed as a function of downstream position as determined from the experimental measured mean velocity profiles

Curve	Froude number	U_1 cm/sec	$X = 109$	$X = 200$	$X = 330$	$X = 440$	$X = 640$	Owen and Gillette (1985)
			cm X/H $= 2.56$ u_* , cm/sec	cm X/H $= 4.58$ u_* , cm/sec	cm X/H $= 7.32$ u_* , cm/sec	cm X/H $= 9.49$ u_* , cm/sec	cm X/H $= 13.6$ u_* , cm/sec	u_* , cm/sec
<i>A</i>	10.4	646	43.9	37.5	39.1	34.3	36.4	33.4
<i>B</i>	13.8	748	47.7	34.8	39.6	43.9	38.6	40.7
<i>C</i>	18.6	866	58.4	56.8	51.4	48.8	48.8	50.0
<i>D</i>	27.6	1060	90.0	79.3	76.1	66.4	64.8	66.6

Note: X is the distance from the leading edge of the tunnel. H is the inside tunnel height (47 cm). U_1 was the inviscid upstream speed. The Froude defined as $U_1^2/(Hg)$

However, for a saltating flow, this focus point is shifted to finite speed, u' , and a different height, k' , called the roughness height in saltation (Bagnold [1]). The speed u' is generally associated with the perceived speed at which the surface particle appears to move.

In order for this phenomenon to be measured, the saltation process must have reached an equilibrium condition, i.e., constancy of u_* as a function of downstream position. The composite velocity profile of Fig. 4 displays this $u' - k'$ phenomenon. At a downstream distance of 640 cm from the beginning of the bed, an easily observed u' of 187 cm/s and k' of 0.22 cm are seen. These values of k' and u' compared reasonably well with the data published by Bagnold ($u' = 250$ cm/sec and $k' = 0.30$ cm), and Zingg [17] who reported $k' = 10d$ and $u' = 895d$, where d is the mean particles diameter in mm and k' and u' are expressed in cm, or for the present case $u' = 224$ cm/s and $k' = 0.25$ cm. Bagnold's mean particle diameter was about 270 microns, while the present experiments diameter was 250 microns.

6 Froude number effect on saltation

For each constant Froude number test, the Froude number was based on the inviscid velocity upstream of the bed, i.e., $Fr = U_1^2/(gH)$. The friction speed was determined as a function of the normalized downstream location for each Froude number case tested and is shown in Fig 5. For a given Froude number, u_* was observed to approach a constant value as the x/H parameter was increased.

A comparison of Fig. 5 with Fig. 4 of Owen and Gillette [11] is appropriate. Owen and Gillette's case considered a smooth surface upwind of the bed thus providing an initial c_f' (or $2u_*^2/U_1^2$) that was lower than the downstream values, however, in the present experiments the upstream value of c_f' was larger than the downwind surface, i.e., the current experiment had no smooth upwind surface. These different set of inlet conditions explain why the Owen and Gillette curves asymptotically increase with increasing downstream distance while the present data decrease with increasing downstream distance.

The current experiments have Froude numbers that range from 10.4 to 27.6, some of which are below the minimum independence number of 20 set by Owen and Gillette. The trends of Fig. 5 suggest that the u_* curves are approaching a constancy value and the smaller the value of Froude number the more rapidly the constancy of u_* is approached. Also shown on Fig. 5 are the asymptotic values of u_* as calculated from the Owen and Gillette theory (see Table 1). The agreement between theory and experiment is remarkable. However, even in the cases where the Froude number was less than 20, it took a minimum x/H

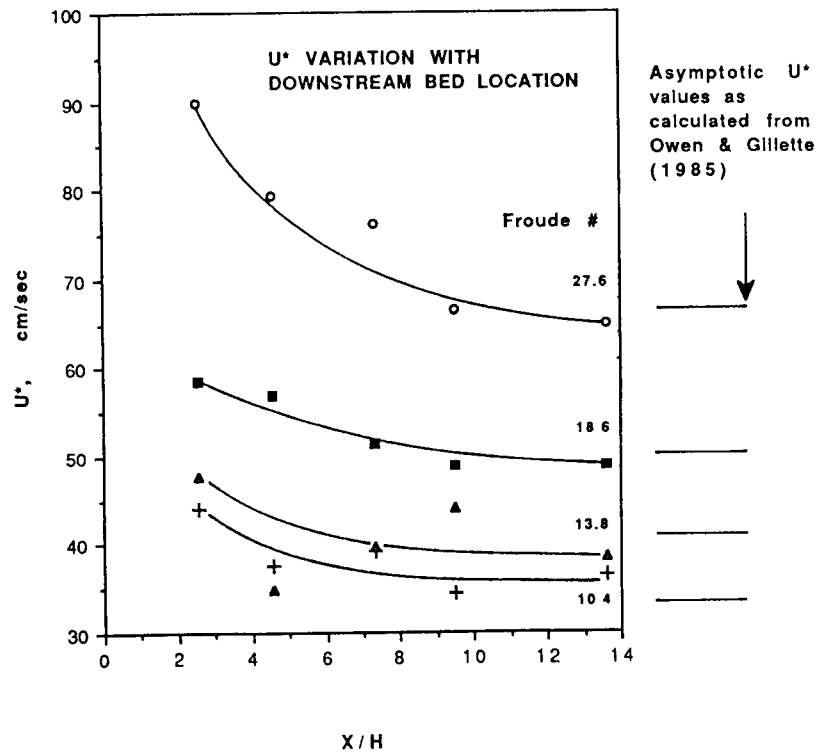


Fig. 5. The friction speed as a function of nondimensional downstream length x/H . Also shown, to the right of the figure, are the predicted values of u_* (Owen and Gillette [11]) as downstream distance becomes large

distance of at least 5 for the u_* -curves to become relatively constant with further changes in downstream position.

The air flow that enters the wind tunnel is initially almost uniform. There is a minimum entrance length required for the velocity deflected layer to resemble a boundary-layer profile. Spires and other boundary layer tripping devices can shorten this entrance length; nevertheless, some minimum length still will be required to obtain a boundary layer velocity profile. The observed minimum x/H value of 5 in the current data illustrates, experimentally, the requirement of this minimum entrance length. For downstream locations less than $5H$, the friction speed has not reached its steady-state value. Consequently, the saltation process has not achieved equilibrium.

Perhaps a more refined measure, instead of x/H , would be x/δ , where δ is the boundary layer height. Generally, an absolute minimum of 25δ is required to produce an equilibrium flow (non-saltating) in terms of mean boundary-layer characteristics, such as the velocity profile (White [13]). Values of x/δ from 50 to 500 are further required to insure an equilibrium flow exists in the more subtle indicators such as turbulence intensities, development of inertial subrange and energy spectra. Fortunately, these more stringent guidelines do not apply directly to saltating flows since the particle motion severely modifies the boundary layer. Nonetheless, 25δ as a minimum entrance length requirement should be adhered to in order to establish equilibrium (constant friction speed) saltation flows. This assumes the Froude number is less than the critical value.

Some previously unpublished (Leach [7] and Iversen [5]) mass transport data from the MARSWIT low-pressure wind tunnel (Greeley et al. [4]), located at NASA Ames Research Center, Moffett Field, California, is also available for consideration. Figure 6 displays a

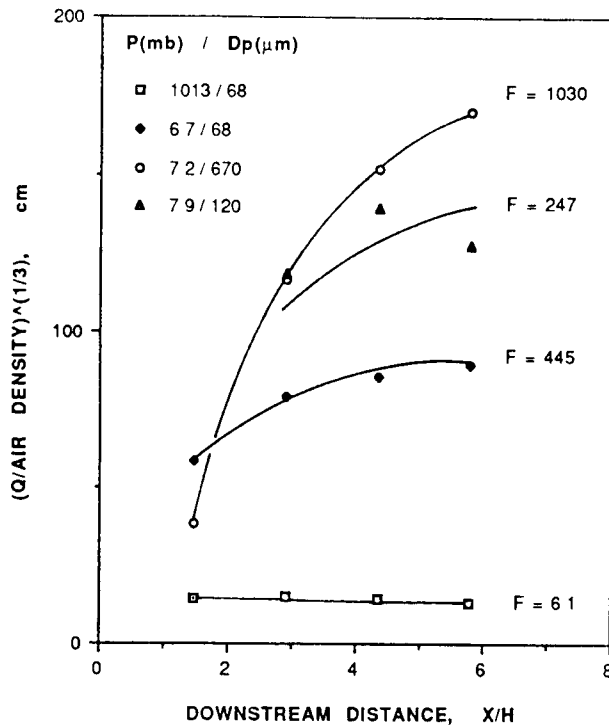


Fig. 6. The NASA MARSWIT wind-tunnel mass collected data as a function nondimensional downstream distance x/H . The Froude numbers vary from 6.1 to 1030. P is the ambient pressure in millibars while D_p is the mean particle diameter in microns, after Iversen [5]

normalized mass collection parameter, $(M/\rho)^{1/3}$, which is proportional to the friction speed, as a function of downstream position for the four Froude number cases tested. Notice, the ambient pressure varies from 1013 mb (atmospheric pressure) to 6.7 mb (low pressure). The low-pressure saltation experiments have relatively higher freestream wind speeds which result in much larger values of Froude number (to order velocity squared). If u_* is constant with downstream distance, then the mass collection parameter, $(M/\rho)^{1/3}$, should also be constant with downstream distance. The observed trends in the data suggest that for large values of Froude number (greater than 100) the friction speed is not constant. Owen and Gillette [11] conclude from their analysis that when the Froude number is greater than 100, saltating particles will collide with the tunnel ceiling which has been observed in the MARSWIT tunnel when operated at low-pressure conditions (see Fig. 5; White [14]). For the atmospheric-pressure case (Froude number equal 6.1) u_* is constant as a function of downstream distance.

In summary, the current data trends suggest there is strong support for the idea put forth by Owen and Gillette of a critical Froude number required for independence of wind-tunnel effects. However, there is a lack of experimental data available to accurately assess the value of this independence Froude number. It seems as though the value of 20 may be liberal and a more conservative value of 10 would further insure a wind tunnel to be free of Froude number effects or constraints. Separately, a minimum entrance length of 25δ is required.

7 Saltating mass as a function of height

The distribution of mass flux as function of height also was measured. The particle collection system consisted of 25 individual 2 cm high, stackable Plexiglas collectors as described in White [14]. Each collector had approximately 2 cm² frontal cross-sectional area and a wire mesh at the back wall which allowed air and mean-sized particles of 40 microns diameter or less to pass through it. The air flow through the rear wall area of the collectors prevented separation from occurring off the sharp-edged intersection of the side wall with the rear wall. Flow visualization studies showed particles to be efficiently trapped. Once the collectors were positioned inside the tunnel and the freestream wind speed achieved, an automated collection system commenced. The length of the collection time for calculation of flux rates was performed by a stop watch with an accuracy of 0.01 seconds. This introduced a negligible uncertainty since collection times were typically greater than 30 seconds. After the particles were caught in the individual traps, the material of each trap was weighed by a Metler scale (accuracy of 0.1 g).

The mass flux as a function of height was measured at a downstream distance of 640 cm; simultaneous measurements of velocity profiles also were performed at the same location, see Fig. 4, $x = 640$ cm. The logarithm of the mass flux was plotted as a function of the height of each collector as shown in Fig. 7. This plot should be expected to trace a straight line, as previous work has shown an exponential dependence of mass distribution with height (White, [14] and others). At higher speeds, the appearance of a linear logarithmic relation is better than it is at lower speeds. This could be attributed to the accuracy of the scale used to measure the mass collected for a particular run. Also, at lower speeds, the uncertainty in the measurements becomes large since the collected mass is small.

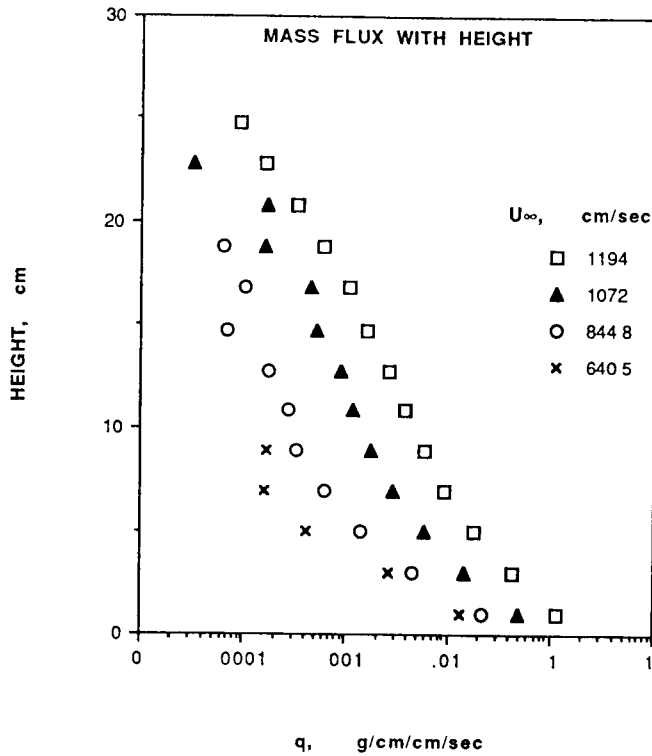


Fig. 7. The logarithm of the mass flux, q , as a function of height for different wind strengths

Nalpanis [9] had proposed that the following relationship be used to describe the exponential dependence of mass distribution with height,

$$q = \alpha e^{-[\lambda q u / u_*^2]}$$

where α and λ are constants for a single experiment. However, Nalpanis concluded based upon analysis of his data that "there does not seem to be any *a priori* way of determining the values of α and λ ". The present data also was fitted to this expression, and, although there are definite tendencies of the data, i.e., λ and α both increasing with increasing u_* values, the same conclusion of Nalpanis was reached for our data. No satisfying equation could be established to account for the α and λ variation from one experiment to another. The α and λ parameters appear not to be constants but rather functions of u_* , particle density and probably functions of particle shape, distribution of particle size and surface roughness. Our values of α ranged from about 30 to 100 mg/(cm² · s), while values of λ varied from unity to about 1.5 both of which uniformly increased with increasing friction speed. The range of α and λ values somewhat agree with the Nalpanis values when the density ratio of walnut shell to sand is accounted for in the λ parameter (our λ 's typically are larger by a factor of 2.5 to 3, the ratio of sand to walnut shell density).

8 Total mass flux collection

The total particle flow consists of the saltation together with the surface creep and a small remainder which may be carried in suspension. The surface creep derives its forward momentum from the bombardment of the impacting saltating particles. It is believed to be

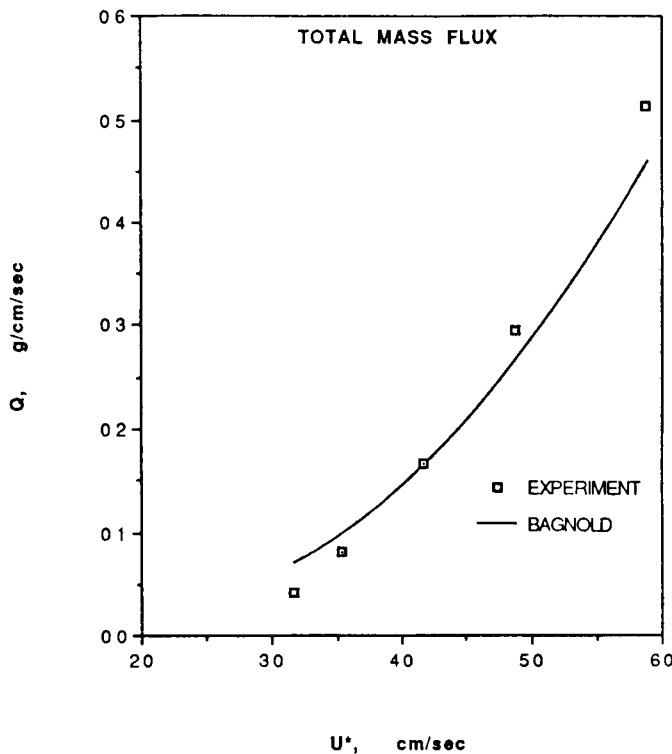


Fig. 8. Total mass flux as a function of friction speed. The solid curve is the theory of Bagnold [1]

approximately equal to a quarter of the total mass transport. The effect of particles in suspension may be safely neglected, except in the case of a very dusty particle flow (particles of 20 microns or less). Accordingly, a 120 mesh screen was used in the construction of the back and top of the total mass flux collector, which was of similar geometric shape as the Section VII collectors without the individual vertical departments, i.e., one single vertical collector which extended to the tunnel flows to the tunnel ceiling. The screens allowed air to pass through the collector and decrease the pressure build-up inside the collector. A 60° angle plate (baffle) was placed inside the collector, at half the distance from the collector leading edge. This baffle helped decrease the pressure build up inside the collector. The angle between the side plate and the perpendicular plate was varied to obtain the optimum collector design for maximum particle collection.

Three different collector angles were tested and flux measurements made and averaged. The freestream velocity was held constant at 900 cm/s during these experiments. It was found that the optimum collector had an angle of 12°, which corresponded to the same angle used in constructing the individual collectors. This value of the angle supported the results obtained for the mass flux as function of height given in Section VII.

The trapped mass was measured by emptying the collector particle mass on the Metler scale plate. The total flux, Q , consisted of the mass passing through a unit vertical width during a measured time. The measured total mass flux was compared to published theories by White [12], Kawamura [6], and Bagnold [1]. The experimental results fell in between these three theories, more closely agreeing with Bagnold's results as shown in Fig. 8. The two other theories gave higher values of the mass flux and generally are expected to be more accurate than Bagnold's equation near threshold conditions since it does not account for zero flux below particle threshold. The discrepancy between the various theories

and data may be explained by the fact that it is known that not all wind-tunnel particle collection systems for total flux determination are accurate or 100% efficient, usually resulting in low mass flux measurements. The shape of the collector is very important in collecting mass fluxes.

9 Concluding remarks

The present study considered several aspects of wind-tunnel saltation including: the effect of Froude number, the determination of mean velocity profiles and friction speeds in saltation as a function of downstream position, saltating mass as a function of height and total mass flux. Most of the experimental measurements were acquired in a relatively small UC Davis boundary-layer wind tunnel. Some previously unpublished MARSWIT wind-tunnel data was also utilized. The Froude number ranged from 6 to 1000.

Some of the major findings are summarized below

- The principle of an independence Froude number (proposed by Owen and Gillette [11]), below which saltation is uninfluenced by the wind tunnel walls, is supported by the present study. However, the value of the critical Froude number may be lower than 20, the value suggested by Owen and Gillette. The present data suggest flows with Froude numbers of 10 or less obtain constant friction speed status more quickly than higher Froude number flows, although it is noted that selection of the critical Froude number is somewhat subjective and may vary among different investigators.
- Additionally, there appears to be a minimum entrance length necessary to develop equilibrium saltation, which is defined as having uniform downstream values of friction speed. Experimentally, it was observed that this distance corresponded to a tunnel length-to-height ratio of at least 5. Moreover, a minimum downstream distance of 25 boundary layer heights is suggested to insure a reasonable developed turbulent boundary layer flow, in the mean flow characteristics only, is present.
- In order to have well defined saltation parameters u' and k' , as defined by Bagnold [1] it was necessary that the saltation process had reached equilibrium. This means that the Froude number must be below the critical value and x/H must be in excess of 5 for u' and k' to exist. This may explain why some previous researchers failed to achieve or observe u' and k' in their wind-tunnel saltation flows.
- The collection of total vertical mass flux was found to be a strong function of the collector geometry giving raise to the validity of these measurements without first investigating the effect of the aerodynamic efficiency of the collector. Present results were found to follow the Bagnold equation reasonably well when the optimum collector shape was used.

References

- [1] Bagnold, R. A.: *The physics of blown sand and desert dunes*. London: Methuen (1941).
- [2] Coles, D.: The law of the wake in turbulent boundary layer. *J. Fluid Mech.* **1**, 191–226 (1956).
- [3] Greeley, R., Iversen, J. D.: *Wind as a geologic process on Earth, Mars, Venus, and Titan*. Cambridge: Cambridge University Press, p. 100 (1985).
- [4] Greeley, R., White, B. R., Pollack, J. B., Iversen, J. D., Leach, R. N.: *Dust storms on Mars*:

- considerations and simulations. In: Desert dust: origin, characteristics, and effect on man. (Perve, T., ed.) Special on Geological Society of America, (1981).
- [5] Iversen, I. D.: Saltation in the wind tunnel. Unpublished manuscript, (1988).
 - [6] Kawamura, R.: Study on sand movement by wind (in Japanese). Institute of Science and Technology, Tokyo University, Tokyo, Report 5, 95–112, (1951).
 - [7] Leach, R. N.: Private communication, (1984).
 - [8] Mounla, H.: Wind-tunnel measurements of mass transport and velocity profiles in saltating turbulent boundary layers. Master of Science Thesis, University of California, Davis (1989).
 - [9] Nalpanis, P.: Saltating and suspended particles over flat and sloping. II. Experiments and numerical simulation. Proceedings on International Workshop on the Physics of Blown. University of Aarhus, vol. I, (1985), pp. 37–66.
 - [10] Owen, P. R.: Saltation of uniform grains in air. *J. Fluid Mech.* **20**, 225–242 (1964).
 - [11] Owen, P. R., Gillette, D.: Wind tunnel constraint on saltation. Proceedings on International Workshop on the Physics of Blown Sand. University of Aarhus, vol. 2. (1985), pp. 253–269.
 - [12] White, B. R.: Soil transport by winds on Mars. *J. Geophys. Res.* **84**, **B8**, 4643–4651 (1979).
 - [13] White, B. R.: Low-Reynolds-number turbulent boundary layers. *J. Fluid Engng.* **103**, 624–630 (1981).
 - [14] White, B. R.: Two-phase measurements of saltating turbulent boundary layer flow. *Int. J. Multiphase Flow* **5**, 459–473 (1982).
 - [15] White, B. R.: Particle dynamics in two-phase flows. Chapter 8 of *Encyclopedia of fluid dynamics*. Houston, Texas: Gulf Publishing Co., (1986) pp. 239–282.
 - [16] White, Frank M.: *Fluid mechanics*, 2nd ed. McGraw-Hill (1986), p. 398.
 - [17] Zingg, A. W.: Wind tunnel studies of the movement of sedimentary material. Proceedings of 5th Hydraulic Conference, Bulletin **24**, 111–135 (1953).

Authors' address: B. R. White and H. Mounla, Department of Mechanical, Aeronautical and Materials Engineering, University of California, Davis, CA 95616, U.S.A.